


RESEARCH

Open Access



# Differential methylation of circulating free DNA assessed through cfMeDiP as a new tool for breast cancer diagnosis and detection of BRCA1/2 mutation

Piera Grisolia<sup>1,2†</sup>, Rossella Tufano<sup>3†</sup>, Clara Iannarone<sup>2</sup>, Antonio De Falco<sup>3</sup>, Francesca Carlino<sup>4,5</sup>, Cinzia Graziano<sup>2</sup>, Raffaele Addeo<sup>6</sup>, Marianna Scrima<sup>2</sup>, Francesco Caraglia<sup>4</sup>, Anna Ceccarelli<sup>7</sup>, Pier Vitale Nuzzo<sup>8</sup>, Alessia Maria Cossu<sup>2,4</sup>, Stefano Forte<sup>9</sup>, Raffaella Giuffrida<sup>9</sup>, Michele Orditura<sup>4</sup>, Michele Caraglia<sup>2,4</sup> and Michele Ceccarelli<sup>1\*</sup> 

## Abstract

**Background** Recent studies have highlighted the importance of the cell-free DNA (cfDNA) methylation profile in detecting breast cancer (BC) and its different subtypes. We investigated whether plasma cfDNA methylation, using cell-free Methylated DNA Immunoprecipitation and High-Throughput Sequencing (cfMeDiP-seq), may be informative in characterizing breast cancer in patients with BRCA1/2 germline mutations for early cancer detection and response to therapy.

**Methods** We enrolled 23 BC patients with germline mutation of BRCA1 and BRCA2 genes, 19 healthy controls without BRCA1/2 mutation, and two healthy individuals who carried BRCA1/2 mutations. Blood samples were collected for all study subjects at the diagnosis, and plasma was isolated by centrifugation. Cell-free DNA was extracted from 1 mL of plasma, and cfMeDiP-seq was performed for each sample. Shallow whole genome sequencing was performed on the immuno-precipitated samples. Then, the differentially methylated 300-bp regions (DMRs) between 25 BRCA germline mutation carriers and 19 non-carriers were identified. DMRs were compared with tumor-specific regions from public datasets to perform an unbiased analysis. Finally, two statistical classifiers were trained based on the GLMnet and random forest model to evaluate if the identified DMRs could discriminate BRCA-positive from healthy samples.

**Results** We identified 7,095 hypermethylated and 212 hypomethylated regions in 25 BRCA germline mutation carriers compared to 19 controls. These regions discriminate tumors from healthy samples with high accuracy and sensitivity. We show that the circulating tumor DNA of BRCA1/2 mutant breast cancers is characterized by the hypomethylation of genes involved in DNA repair and cell cycle. We uncovered the TFs associated with these DRMs

<sup>†</sup>Piera Grisolia and Rossella Tufano contributed equally to this work.

Michele Caraglia and Michele Ceccarelli co-senior authors.

\*Correspondence:  
Michele Ceccarelli  
m.ceccarelli@gmail.com

Full list of author information is available at the end of the article



© The Author(s) 2024. **Open Access** This article is licensed under a Creative Commons Attribution-NonCommercial-NoDerivatives 4.0 International License, which permits any non-commercial use, sharing, distribution and reproduction in any medium or format, as long as you give appropriate credit to the original author(s) and the source, provide a link to the Creative Commons licence, and indicate if you modified the licensed material. You do not have permission under this licence to share adapted material derived from this article or parts of it. The images or other third party material in this article are included in the article's Creative Commons licence, unless indicated otherwise in a credit line to the material. If material is not included in the article's Creative Commons licence and your intended use is not permitted by statutory regulation or exceeds the permitted use, you will need to obtain permission directly from the copyright holder. To view a copy of this licence, visit <http://creativecommons.org/licenses/by-nc-nd/4.0/>.

and identified that proteins of the Erythroblast Transformation Specific (ETS) family are particularly active in the hypermethylated regions. Finally, we assessed that these regions could discriminate between BRCA positives from healthy samples with an AUC of 0.95, a sensitivity of 88%, and a specificity of 94.74%.

**Conclusions** Our study emphasizes the importance of tumor cell-derived DNA methylation in BC, reporting a different methylation profile between patients carrying mutations in BRCA1, BRCA2, and wild-type controls. Our minimally invasive approach could allow early cancer diagnosis, assessment of minimal residual disease, and monitoring of response to therapy.

**Keywords** Breast cancer, Cell-free DNA, DMRs, cfMeDIP-seq, BRCA1, BRCA2

## Background

Breast Cancer (BC) is the most common cancer in women all over the world. It differs in histological and molecular characteristics that, in turn, influence the clinical outcome and response to therapy of the patients [1]. Genetics, carcinogen exposure, physical activity, and hormonal levels are the main risk factors. Most BCs arise from genetic and epigenetic somatic mutations, while approximately 5% of all BC is caused by germline mutations. BRCA1 and BRCA2 are the most frequent genes associated with an increased risk of BC occurrence. They are involved in DNA homologous recombination repair (HRR) and, thus, crucial to repair DNA double-strand breaks during S/G2-Phase.

Moreover, BRCA2 is involved in maintaining the stability of stalled replication forks [2] and is necessary to assure genetic integrity upon chemotherapy exposure. The loss of function in BRCA1 and BRCA2 genes leads to an activation of less precise repair pathways that would result in more errors and accumulation of DNA damage [3]. The risk of developing BC arises up to 75% in women carriers of BRCA1 and BRCA2 mutations characterized also by a more aggressive phenotype if compared to sporadic tumors [4]. BRCA1/2 mutated BCs often have a triple-negative phenotype (lack of expression of estrogen, progesterone, and ErbB2 receptors). Patients with this subtype have a worse prognosis and require specific personalized treatments that especially involve the use of immune checkpoint inhibitors (ICIs) such as pembrolizumab and/or Poly (ADP-ribose) polymerase (PARP) inhibitors such as Olaparib [4]. Moreover, a germline mutation of BRCA1 or BRCA2 predicts a high response rate to platinum and its derivatives [5]. Therefore, the precise definition and detection of BRCA1 or 2 mutated BC patients should deserve particular attention for the best choice of therapy and the correct clinical management of the patients.

Epigenetic modifications are considered a hallmark of cancer and are found in the early stages of disease, tumor progression, and metastasis formation. DNA methylation is a tissue- and cancer-specific modification and, in contrast to the heterogeneity of gene mutations, appears to change similarly in cancer cells of the same type and

tissue origin [6, 7]. The methylation profiles in BCs may differ according to both the diverse BC molecular subtype and the presence of BRCA gene mutations. Indeed, there are differences in the methylome of patients with pathogenic germline BRCA mutations compared with familial BC without BRCA mutation [8]. BRCA1 mutated patients have lower methylation abundance than those with sporadic tumors [9]. Moreover, it is often difficult to predict the pathogenicity of the so-called variants of unknown significance (VUS), and longer clinical observation of these individuals is needed to define their involvement in the disease occurrence [10]. In these cases, the methylation data alone could be helpful to predict the pathogenicity of the BRCA variants [11]. The study of the circulating methylation profile in cancer patients can be performed due to the presence of circulating-free DNA (cfDNA) in the plasma. cfDNA comprises small fragments with a mean average size of 167 bp released in the bloodstream by both normal and tumor cells through different processes, including apoptosis, necrosis, and active secretion. The study of cfDNA methylation allows the detection of different cancer types at various stages [12], including BC. Genome-wide methylation analysis by the bisulfite conversion method of cfDNA was used for the early detection of BC [13]. However, this method is expensive, time-consuming, and requires large amounts of cfDNA from plasma. An innovative and highly sensitive alternative arises from utilizing cell-free methylated DNA immunoprecipitation by anti-5mC antibodies and subsequent high-throughput sequencing (cfMeDIP-seq) [14] to assess the methylation profile despite low cfDNA input. Differentially methylated regions (DMRs) have been used to construct classifiers that can identify patients with renal cell carcinoma [14], discriminate between patients with localized and metastatic prostate cancers [15], and diagnose BC [16]. Although different previous papers report the role of cfDNA methylation in different subtypes of BC, it remains unclear how the methylation profile varies in the cfDNA of patients carrying BRCA1 and BRCA2 gene variants.

In the present study, through a minimally invasive, inexpensive, and highly sensitive method, We examined the cfDNA methylation profile in BC patients

with germline BRCA1/2 mutations and BRCA1/2wt, tumor-free, and healthy individuals as reference. Thus, we applied cfMeDIP-seq using plasma-derived cell-free DNA, identified differential methylation profiles in our BRCA1/2mut BC patients, and contextualized these hypo- and hypermethylated regions to publicly available TCGA-BRCA data. Lastly, we translated our findings to establish classifiers to discriminate BRCA1/2mut BC patients from BRCA1/2wt healthy references.

## Methods

### Samples collection

Samples were collected from Azienda Ospedaliera Universitaria Vanvitelli of the University of Campania “L. Vanvitelli,” Presidio Ospedaliero of San Felice a Cancello (Caserta), and “San Giovanni di Dio” Hospital of Frattamaggiore (ASL Napoli 2 Nord). The study was in accordance with the Institutional Ethics Committee guidelines, Italian law, and the Declaration of Helsinki and was approved by the Ethics Committee of University of Campania “Luigi Vanvitelli” - Azienda Ospedaliera Universitaria “Luigi Vanvitelli” - AORN “Ospedali dei Colli” (Approval number: 133449 on 29th April 2021). Informed consent was obtained from all patients. We included 23 BC patients with germline mutation of BRCA1 and BRCA2 genes, 19 healthy controls without BRCA1/2 mutation, and 2 healthy individuals who carried BRCA1/2 mutations (Table 1). Ten mL of peripheral blood was collected in EDTA-containing tubes at the moment of BC diagnosis. Plasma was isolated by centrifugation at 1200 x g for 20 min, followed by a second

centrifugation at 21,300 x g for 20 min, and the supernatant was stored at -80 °C until processing.

### Cell-free DNA isolation and quantification

cfDNA was isolated from 1mL of plasma for each sample by using the Qiaamp Circulating Nucleic Acid Kit (Qiagen) and eluted with 50 µL of Qiagen Elution Buffer. The extracted cfDNA was stored at -20 °C. The concentration of cfDNA was evaluated using Qubit flex fluorometer (ThermoFisher) with Qubit 1X dsDNA High Sensitivity (HS) kit. cfDNA was examined by capillary electrophoresis utilizing a 2100 Bioanalyzer Biosystem (Agilent) and dsDNA High sensitivity kit and chips.

### cfMeDIP-seq

cfMeDIP-seq was conducted following previously published protocols [14]. In short, cfDNA libraries were generated using the Kapa Hyper Prep Kit (Roche) according to the manufacturer’s guidelines. After performing end-repair and A-tailing, adaptors from the NEBNext Multiplex Oligos for Illumina (NEB) were ligated to the samples, followed by purification using AMPure XP beads. To achieve a final quantity of 100 ng, Lambda DNA—comprising both methylated and unmethylated amplicons with varying CpG content—was added to the libraries. 0.3 ng of methylated and unmethylated *Arabidopsis thaliana* DNA was added for quality control purposes (Diagenode). One small part of the library was kept aside for input control (IC), and the remaining was used for immunoprecipitation (IP). MeDIP was carried out with the MagMeDIP Kit (Diagenode), Antibody anti-5mC\* (33D3 clone) as per the manufacturer’s protocol. The efficiency of the immunoprecipitation was verified via qPCR by detecting the recovery of the spiked-in *Arabidopsis thaliana* DNA (both methylated and unmethylated), following Diagenode’s instructions, and all samples with a specificity of reaction <99% were excluded from the study. All final libraries (IC and IP) were amplified using between 9 and 15 cycles assessed by qPCR following the cfMeDIP-seq protocol, with the following protocol: 98 °C for 3 min, 98 °C for 20s, Anneal at 65 °C for 15s and Extension at 72 °C for 30s. After amplification, libraries were purified, leading to a dual-size selection with AMPure XP beads (Beckman Coulter). Library quality was examined by capillary electrophoresis utilizing a 2100 Bioanalyzer Biosystem (Agilent) and dsDNA High-sensitivity kit and chips.

### Sequencing

Whole genome sequencing (WGS) was performed for pre-made libraries at Novogene Company (Cambridge) on Novaseq6000 (Illumina) with a 150PE. The mean total reads for the IP samples were 32.8 million per sample resulting in ~3X depth per sample. IC samples were

**Table 1** Clinical pathological characteristics of the patient’s cohort

Clinical pathological characteristic	Tumoral BRCA+ (n:23)	Controls BRCA- (n:19)	Controls BRCA+ (n:2)
<b>Age (mean)</b>	50.1	45.5	34.5
<b>Sex</b>	23	19	1
F	-	-	1
M			
<b>BRCA status</b>	10	-	1
BRCA1	13	-	1
BRCA2			
<b>Stage</b>	16	-	-
Localized (I-III)	7	-	-
Metastatic			
<b>Grade</b>	1	-	-
I	10	-	-
II	12	-	-
III			
<b>Breast Cancer Subtype</b>	13	-	-
Luminal-Like	9	-	-
TNBC	1	-	-
HER2			

sequenced at the resolution with a mean of 54.7 million per sample resulting in ~5.1X depth per sample.

#### Processing of cfMeDIP-seq data

The quality of raw reads was evaluated using FastQC version 0.11.9 (<https://www.bioinformatics.babraham.ac.uk/projects/fastqc>) and MultiQC version 1.11 [17]. Then, low-quality reads and adaptors were removed with Trim Galore version 0.6.6 ([https://www.bioinformatics.babraham.ac.uk/projects/trim\\_galore](https://www.bioinformatics.babraham.ac.uk/projects/trim_galore)). The trimmed reads were aligned to hg38 with Bowtie2 version 2.3.4.3 [18]. SAMTools version 1.9 [19] was used to convert the SAM alignment files to BAM files, sort and index reads, and remove duplicates. Samples with <10 M mapped reads were excluded. Tumor fraction was estimated using IchorCNA [20] on the low-pass WGS of IC samples.

#### Identification and annotation of differentially methylated regions (DMRs)

The filtered BAM files were processed using MEDIPS [21] to identify the Differentially Methylated Regions (DMRs) between BRCA1/2mut breast cancer patients and healthy non-carriers. The enrichment scores relH and GoGe were estimated for each sample to express the grade of CpG enrichment in the DNA fragments compared to the reference genome. The enrichment score relH is the ratio between the relative frequency of CpGs within the regions and the reference genome. The enrichment score GoGe is the observed/expected ratio of CpGs within the regions and the reference genome. Samples with relH less than 2.7 and/or GoGe less than 1.75 were excluded. Then, the genome of each sample was binned into 300-bp windows, and the methylation status of each bin was compared between the two groups. Regions with an absolute value of log<sub>2</sub> fold change (FC) greater than or equal to 2 and a p-value less than 0.01 were selected as differentially methylated. The identified DMRs were annotated with the annotatr [22] R package. Gene set enrichment with DAVID [23] and gene ontologies with a p-value less than 0.05 were selected.

#### Validation of DMRs with the TCGA-BRCA cohort

Methylation data of The Cancer Genome Atlas (TCGA) BRCA cohort were downloaded with the *TCGABiolinks* R package [23]. The primary tissue profiled for BRCA and solid tissue normal were downloaded. We referred to the cBioPortal for Cancer Genomics (<http://www.cbioportal.org>, accessed on 23 October 2023) to assess the TCGA-BRCA samples profiled for germline BRCA1/2 mutations. The probes of Infinium HumanMethylation450K Bead-Chip array that overlapped with the previously identified DMRs were selected to perform a Principal Component Analysis (PCA). Overlapping probes were identified with findOverlaps of R package GenomicAlignments [25].

#### Motif finding

Motif enrichment analysis was performed with the HOMER tool [24] on two sets of DMRs: (1) hypermethylated DMRs and (2) hypomethylated DMRs. A BED file for each set was built. The motifs with a p-value lower than 0.05 were selected for downstream analysis.

#### Transcription factor enrichment analysis

We inferred the protein activities using VIPER [25]. We used the expression data of 82 samples of the TCGA-BRCA cohort, of these 41 primary tissue samples harboring germline BRCA1/2 mutations and 41 normal tissue samples randomly selected, and the BC transcriptional regulatory network generated by ARACNe-AP [26]. We used the *aracne.networks* R package to download the BC interactome. Then, we estimated the differential activity of regulatory proteins between primary and normal tissue samples by applying the Student's t-test to the values of protein activities inferred from their expression level and selected as dysregulated transcription factors with false discovery rate less than 0.05 and an absolute value of delta greater or equal than 1.

#### Classification of the samples by using the DMRs

Identified DMRs were used to train two different classifiers, one based on the GLMnet model and the other one on a random forest machine learning algorithm. In both cases, the adopted cross-validation method was the leave-one-out cross validation (LOOCV). Caret was used for sample classification, while the ROCR [27] was used to estimate the area under the curve (AUC). We estimated the optimal cut-off for each classifier by applying the Youden Index (J) method [28].

## Results

#### Cell-free DNA quantification in BRCA mutation carriers

As a first quality check, we evaluated the detectable cfDNA quantity from plasma in our cohort. For each sample, cfDNA isolation was performed starting from 1 mL of plasma, and the final elution of cfDNA was made in 50µL of AVE buffer to have the same starting conditions. Fluorometric quantification was performed by a spectrofluorometer that automatically releases the concentration of dsDNA based on the fluorescence emitted by a specific DNA-binding dye. The mean concentration of cfDNA in patients with BRCA1/2 germline mutations was 0.344 ng/µL, while the mean concentration of cfDNA from healthy controls without mutations was 0.198 ng/µL. There was a statistically significant difference between the two groups (p-value 0.032, two tails t-test) (Supplementary Figure S1). These results show that tumor samples of BRCA1/2 carriers tend to have a higher amount of detectable cfDNA with respect to healthy controls.

**Identification of differences in methylation profile between BRCA1/2 germline mutation carriers and non-carriers healthy patients**

We investigated the differences in the methylation profile extracted from the cfDNA using the cfMeDIP-Seq protocol between 25 BRCA germline mutation carriers and 19 healthy non-carriers. These samples were selected after quality checking on the basis of the number of mapped reads and enrichment scores. We performed low-pass

whole genome sequencing on immuno-precipitated samples as described in the Methods. The average number of the mapped reads was 28.7 million, with a standard deviation 15.3. We identified 7,095 hypermethylated and 212 hypomethylated 300-bp regions ( $|\log_2 FC| \geq 2$  and  $p\text{-value} < 0.01$ ) and observed a more significant proportion of DMRs in hypermethylated regions with respect to hypomethylated regions (97% vs. 3%,  $p\text{-value} < 2.2e-16$ ) (Fig. 1A).

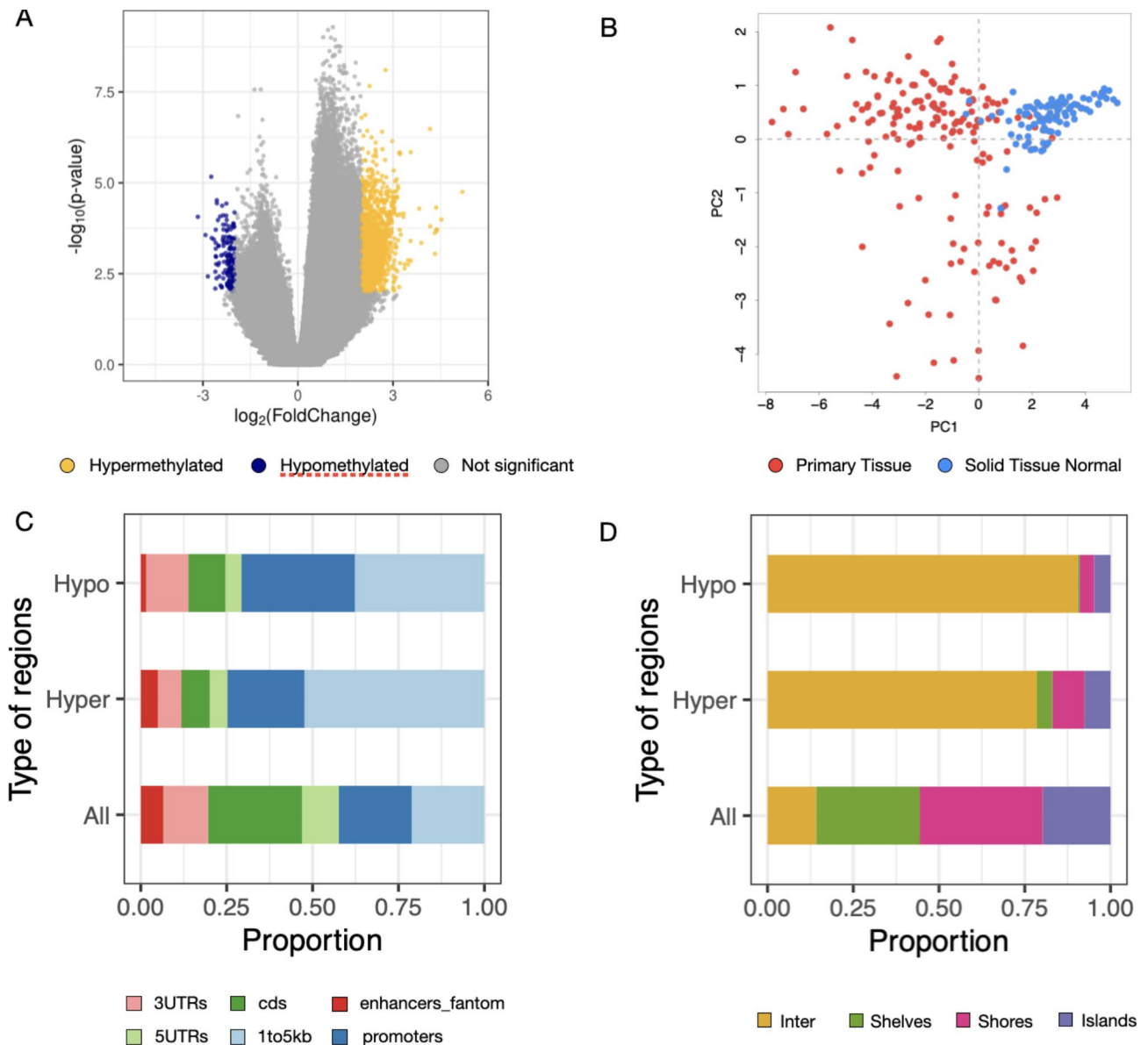


**Fig. 1** Identification and annotation of Differentially Methylated Regions (DMRs). **(A)** The volcano plot shows the DMRs. The x-axis represents the log2 fold change (FC) of methylation, and the y-axis represents the  $-\log_{10}(p\text{-value})$ . The regions with a  $p\text{-value} < 0.01$  and  $|\log_2(FC)| \geq 2$  were selected as differentially methylated. The yellow points represent the hypermethylated regions (7,095), the blue points represent the hypomethylated regions (212), the dark gray points represent the not significant regions. **(B)** Principal Component Analysis of TCGA-BRCA methylation data overlapping the DMRs. The red points represent the primary tissue samples, while the blue ones represent the solid tissue normal samples. **(C)** Proportion of DMRs according to Genic Annotations. The distribution of DMRs across the 3UTRs (3' untranslated regions), CDS (coding DNA sequences), enhancers\_fantom (enhancers from FANTOM5), 5UTRs (5' untranslated regions), 1to5kb (1 to 5 kb regions upstream of transcription start site, TSS), promoters (regions with a length of less than 1 kb upstream of TSS) were explored. **(D)** Proportion of DMRs according to CpG Annotations

To understand if the identified DRMs are cancer-related, we used the methylation status of a group of samples from the TCGA dataset over the identified DMRs. We selected normal solid tissues and primary BC tissue samples profiled for BRCA germline mutations. We selected the probes of the Infinium Human Methylation 450 K BeadChip array in the TCGA-BRCA cohort that overlapped with the identified DMRs in cfMeDIP-seq experiments and performed a principal component analysis (PCA) on this set of probes. We observed that the PC1 over the identified DMRs was able to separate the primary BC samples from normal solid breast tissue samples (Fig. 1B). This result confirms that patients with BRCA mutations show an altered methylation profile that correlates with BC occurrence [8]. Interestingly, the same BRCA-specific methylation phenotype can be detected even in cfDNA.

To explore the biological effects of the identified DMRs, we evaluated the percentages of specific genetic loci affected by methylation changes. According to the genic annotation, we explored the distribution of the DMRs across the 3' untranslated regions (3UTRs), the coding DNA sequences (CDS), the enhancers from FANTOM5, the 5' untranslated regions (5UTRs), the 1 to 5 kb regions upstream of transcription start site (TSS), the promoters (regions with a length of less than 1 kb upstream of TSS). We observed that hypermethylated and hypomethylated regions were mainly located in 1 to 5Kb upstream of the TSS and promoter regions and higher than expected with respect to the set of considered regions (Fig. 1C). We found 52% of hypermethylated regions ( $p$ -value  $< 2.2 \times 10^{-16}$ , proportion test) and 37% of hypomethylated regions ( $p$ -value  $6.769 \times 10^{-6}$ , proportion test) were located in 1 to 5Kb upstream of the TSS compared to 21% of considered regions of the genome. In addition, we observed that the proportions of both hypermethylated and hypomethylated regions in the CDS and 5'UTRs were reduced compared to the expected proportions. 5% of both hypermethylated ( $p$ -value  $< 2.2 \times 10^{-16}$ , proportion test) and hypomethylated regions ( $p$ -value  $0.03446$ , proportion test) were located at 5'UTR regions compared to the 11% expected by chance. The proportion of regions in CDS was 8% for the hypermethylated regions ( $p$ -value  $< 2.2 \times 10^{-16}$ , proportion test) and 11% for the hypomethylated regions ( $p$ -value  $3.509 \times 10^{-5}$ , proportion test) compared to 27% of the regions in the whole genome. In contrast, the proportion of the regions at 3'UTRs was almost similar ( $p$ -value  $0.9163$ , proportion test) in the hypomethylated regions (12%) versus the expected (13%), while the proportion observed across the hypermethylated regions was 7% ( $p$ -value  $< 2.2 \times 10^{-16}$ , proportion test).

We also observed that both hypermethylated and hypomethylated regions were preferentially located in intergenic regions in contrast with the expected proportion

observed in the whole genome (Fig. 1D). In particular, 90% of hypomethylated regions were in intergenic regions with respect to an expected 14% ( $p$ -value  $< 2.2 \times 10^{-16}$ , proportion test). Overall, this analysis shows that differential methylation of cfDNA between BRCA1/2 patients and healthy controls is not random but rather, it is enriched in regulatory regions of the genome.

#### Biological mechanisms of differential methylation in BRCA1/2 mutation carriers

Biological Process (BP) enrichment analysis of genes annotated in the hypermethylated and hypomethylated regions was performed, resulting in 25 significant categories ( $FDR < 0.05$ , Fisher's Exact test) activated in the hypermethylated regions. In contrast, no BP was significantly enriched in hypomethylated regions (Supplementary Table S1).

We found enriched categories related to signal transduction, polymerase II promoter, cell adhesion, neuronal development, vasculogenesis, and potassium by using the hypermethylated regions in the BRCA mutation carriers (Fig. 2). Among the GTPases we found hypermethylation of tumor suppressors related to Rho and RAS GTPase activities such as DLC1 and STARD13, which play key roles in the regulation of Rho signaling and cytoskeleton remodeling [29], and RASA1 whose gene product stimulates the GTPase activity of normal RAS [30]. Several genes enriching the pathway of regulation of signal transduction mediated by small GTPases had hypermethylated regions in their promoters (Supplementary Table S2). They include ARHGAP21, ARHGAP40, ARHGAP5, the G protein subunit beta 5 GNB5, and the Ras association domain family member 1 RASSF1. These results implied that GTPase activity, and, in particular, related to RHO/RAS activity, could be highly significant in BC with BRCA mutations.

To better characterize the difference between BC and healthy controls, a focused analysis was performed, selecting patients with the highest tumor fraction ( $n = 10$ , range 0.01–0.1) and comparing them with a sample of control cases of the same size. The analyses were performed in the same way as previously described. The results were almost similar to the previous ones with the whole cohort but with some differences. There was a greater difference in the overall methylation, as we found 11,0575 of hypermethylated DMRs and 3384 of hypomethylated DMRs in 300-bp regions (77% vs. 23% respectively) (Supplementary Figure S2A). We also observed that the first two principal components could separate primary BC samples from normal solid breast tissue samples more accurately (Supplementary Figure S2B). In addition, like the previous analysis, we observed that hypermethylated and hypomethylated regions were mainly located 1 to 5Kb upstream of the TSS and

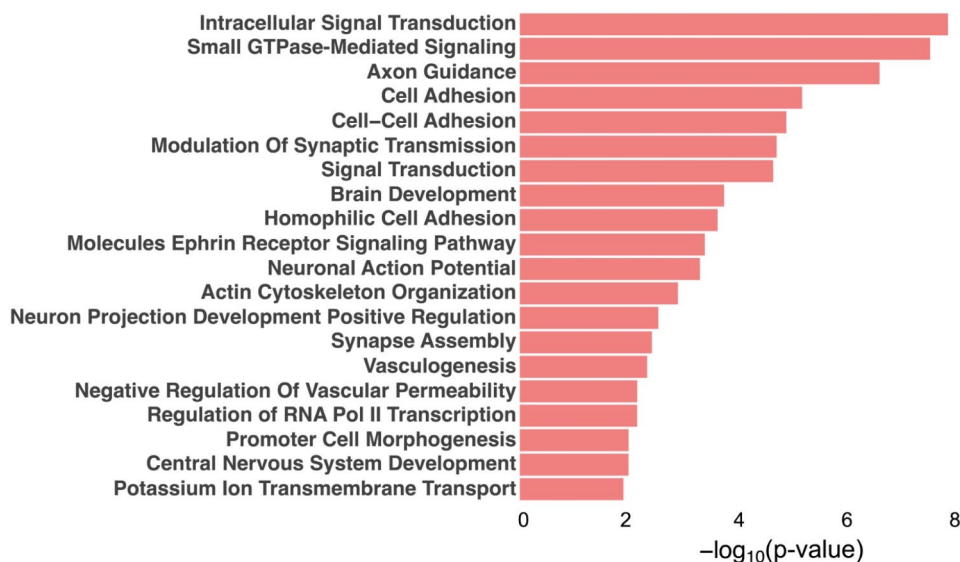


**Fig. 2** Functional annotation of hyper-DMRs in BRCA-carriers Top 20 biological processes enriched by the genes overlapping hypermethylated regions in BRCA-carriers and selected according to p-value. The x axis corresponds to  $-\log_{10}(p\text{-value})$ , and the Y axis corresponds to the gene ontology terms

promoter regions, higher than expected compared with the set of regions considered previously. Furthermore, the proportions of hypermethylated and hypomethylated regions in the CDS, 5'UTR and 3'UTR, were reduced compared to the expected proportions (Supplementary Figure S2C). Finally, we observed that both hypermethylated and hypomethylated regions were preferentially located in intergenic regions, in contrast to the expected proportion observed in the whole genome (Supplementary Figure S2D).

Biological Process (BP) enrichment analysis of genes annotated in the hypermethylated (Supplementary Table S3) and hypomethylated (Supplementary Table S4) regions was performed, as before. The top categories corresponding enriched by the Hyper-methylated regions overlapped the previous findings (Supplementary Figure S3), whereas the BP categories enriched by the hypomethylated regions included immune response signaling pathway, DNA repair, cell cycle and estrogen receptor signaling pathway (Supplementary Figure S3, Supplementary Table 4). Among genes involved in DNA repair mechanisms we found: RFC3, PARP4, RFC1, EYA4, ACTL6A, FANCA, TFPT, UBE2W, RAD50, SUMO1, RRM2B, ERCC4, UBR5, SHLD1, ERCC6, ATR. Collectively, these results show that the circulating tumor DNA of BRCA1/2 mutant breast cancers is characterized by the hypomethylation of genes involved in DNA repair and cell cycle.

#### Regulatory role of differentially methylated regions

To uncover the effect of the BRCA mutation on gene regulation, we performed an enrichment motif analysis using the identified DMRs to evaluate which

transcription factors (TFs) could be affected by the differential methylation. We analyzed the hyper-DMRs and hypo-DMRs separately. In the first case, we found the motifs for 14 TFs enriched ( $p\text{-value}$  lower than 0.05) (Fig. 3A), while we did not find motifs in the hypomethylated (Supplementary Table S5). To evaluate the potential functional effect of the TF activity, we used Viper [25] to infer the TF activity by their expression levels in 82 samples from the TCGA-BRCA cohort (see Methods). Of these, 41 tumor samples carried germline BRCA mutations and 41 solid tissue normal samples. Supervised analysis between the two groups resulted in 610 TFs with an increased activity and 766 TFs with a decreased activity. We selected as dysregulated the TFs with an absolute value of delta greater or equal to 1 and False Discovery Rate (FDR) lower than 0.05 (Fig. 3B, Supplementary Table S6). We found that DMRs enriched binding motifs of 4 dysregulated TFs (ERG, FLI1, ETS1, RUNX1) with a decreased activity.

Overall, our results identified TFs belonging to the ETS and RUNX transcription factor family and in particular, ETS1, ERG, and FLI1 are associated with BRCA1/2 mutated breast cancer.

#### Development of classifiers based on DMRs

To explore the potential clinical application of our data, we trained statistical classifiers to check if the identified DMRs can discriminate between BRCA1/2mut BC patients and BRCA1/2wt tumor-free patients based on the cfDNA methylation status. The identified DMRs were used to train statistical classifiers (Fig. 4).

We developed two classifiers. The first was based on the GLMnet model and exhibited high accuracy in cancer

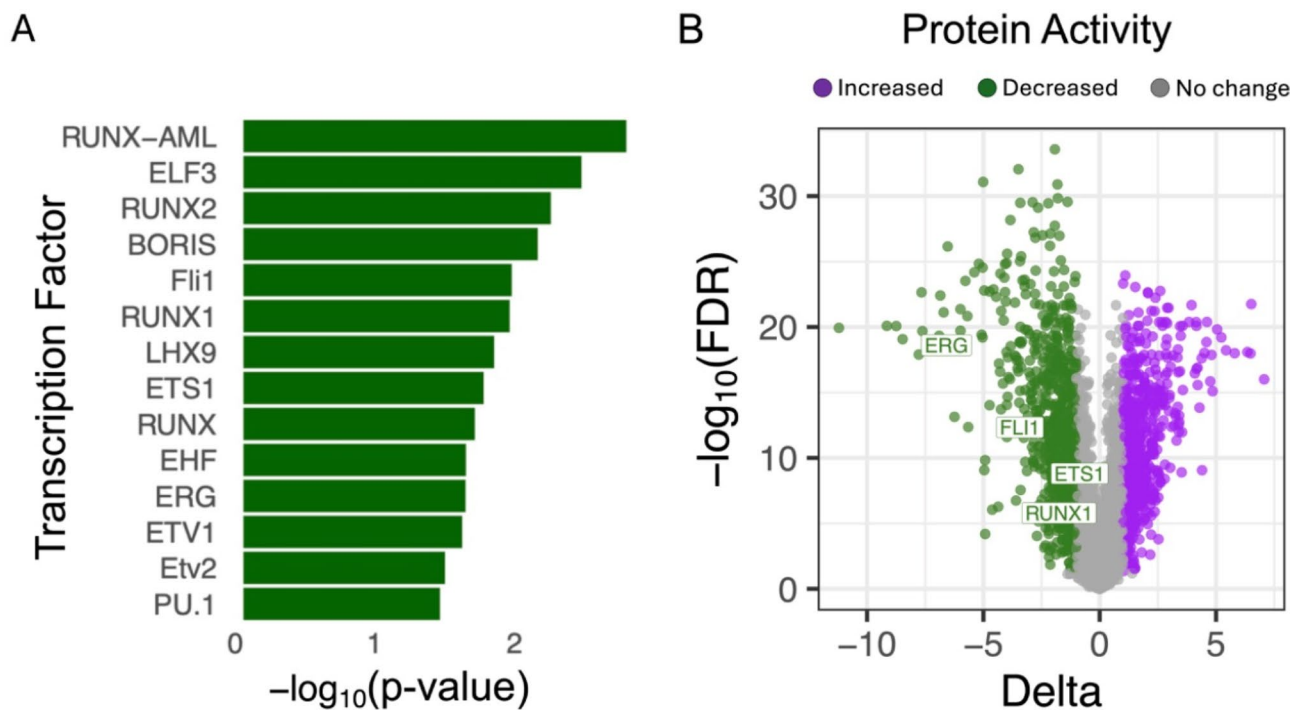


**Fig. 3** Transcription factor enrichment analysis. **(A)** Barplot of enriched binding motifs (y-axis), ordered based on  $-\log_{10}$  p-value (x-axis), encoded by the hyperDMRs **(B)** Volcano plot shows the differentially active TFs estimated comparing 41 BRCA+ tumor samples versus 41 solid tissue normal tissue samples of the TCGA-BRCA cohort. The positively dysregulated TFs are shown in red while the negatively dysregulated TFs are shown in green. The TFs with an absolute value of delta greater or equal to 1 and False Discovery Rate (FDR) < 0.05 were selected as dysregulated. The dysregulated TFs identified with VIPER and HOMER were labeled in the volcano plot

detection, with an AUC of 0.92, a sensitivity of 92%, and a specificity of 94.74%. The second one was based on the random forest model and achieved an AUC of 0.95, with a sensitivity of 88% and a specificity of 94.74%. In both cases, we were able to correctly assign the samples to their group using the optimal cut-off by applying the Youden index (J) method, reporting a value of 0.26 for the first model and 0.51 for the second.

## Discussion

Tissue biopsies and the following pathological examination of the tissues are consolidated procedures for histologic and molecular characterization of tumors. However, they are invasive and often induce discomfort in the patients. Based on these considerations, the relevance of liquid biopsy in both the detection and molecular definition of cancer, including BC, is continuously rising [31]. In fact, liquid biopsy is easy, induces minimal risks for the patients, and can be repeated at different times, allowing the continuous monitoring of the disease over time, determining the changes of the molecular characteristics of the cancer during the treatment of the patient [33, 34]. Epigenetic modifications occur in the earliest stages of the disease in breast cancer [32]. DNA methylation is cancer- and tissue-specific and, therefore, enables the identification of the target tissue origin of

tumors. So, when paired with other biomarker or imaging-based methods, methylation patterns can provide high predictive accuracy for detecting cancer [33]. Several studies have been conducted on cfDNA methylation for early detection of breast cancer [34, 35] and in samples collected prior to clinical detection [36] also through the cfMeDIP-seq (16). This methodology was also used for the detection and discrimination of intracranial tumors [37], to distinguish localized and metastatic prostate tumors [15] and for the molecular residual disease (MRD) detection in head and neck cancer (HNC) [38]. The presence of mutations in the BRCA1 and BRCA2 genes, essential for maintaining genomic stability through their function in DNA repair, increases the risk of breast cancer presenting very early and with increased aggressiveness. In this study, we investigate, by cfMeDIP-seq, the characteristics of the methylome in breast cancer patients carrying mutations in BRCA genes, suggesting blood-based DNA methylation markers serving as potential novel screening markers. As a validation of the differentially methylated regions identified in cfDNA, we have reported that those regions can distinguish TCGA BRCA breast tissues from healthy controls with high accuracy in an unsupervised way.

Among the dysregulated signaling pathways, we identified the role of small GTPase, including some tumor



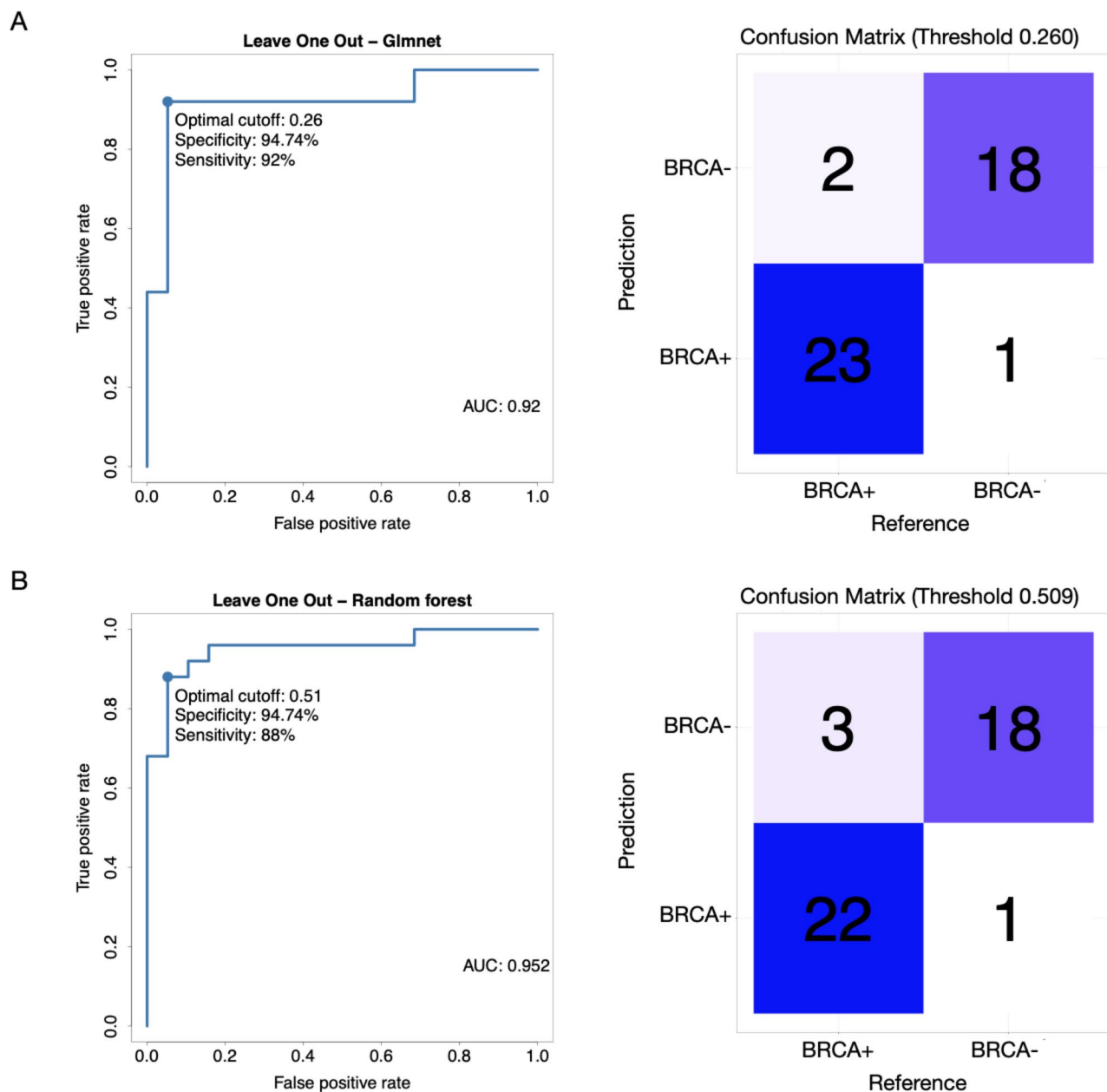


**Fig. 4** Performance of classifiers built using the DMRs as selected features. **(A)** Performance of the classifier based on the GLMnet model **(B)** Performance of the classifier based on the random forest model

suppressors related to Rho and RAS GTPase activities, such as the hypermethylation of promoter of tumor suppressor gene RASSF1, involved in cancer-related pathways such as the Rho/Ras GTPase and Hippo pathway [39]. Moreover, the activity of the transcription factors in 82 samples from the TCGA-BRCA cohort, 41 carried germline BRCA mutations and the remaining 41 adjacent solid tissue normal samples. We identified TFs belonging to the ETS family. Several studies have shown the role of ETS family's member (ETS1, FLI1, and ERG) in DNA damage repair mechanisms [40–42]. Specifically, ETS1

interacts with two DNA repair enzymes, PARP-1 (Poly [ADP-ribose] polymerase 1) and DNA-PK (DNA-dependent protein kinase), and its expression levels appear to be regulated by PARP1. PARP1 inhibition, indeed, leads to increased ETS1 expression with accumulation of DNA damage and cancer cell death [43].

From a focused analysis of differentially methylated regions (DMRs) in samples with the highest tumor fraction we found genes in the hypomethylated regions enriched pathways associated with DNA repair pathway and cell cycle regulation. Among the genes that enriched

these pathways we identified: ATR, ATM, RAD50, PARP4, FANCA. These genes control genomic stability and participate in processes of DNA damage response (DDR), damage tolerance process, and cell cycle checkpoint [44].

The (MRE11-RAD50-NBS) MRN complex, of which RAD50 is an essential component, plays a key role in the DNA damage response (DDR). It primarily recognizes DNA double-strand breaks (DSBs), interacts with ATM (ataxia-telangiectasia mutated) and ATR (ATM- and Rad3-Related) kinases, and forms a complex with BRCA1 to promote the resection of 5' ends in the early stages of the homologous recombination (HR) process [45]. ATM and ATR instead are the most upstream DDR kinase and are involved in phosphorylating several effector proteins downstream of DDR, including histone H2AX and the cell cycle checkpoint proteins p53, CHK1, and CHK2, which promote cycle arrest to prevent replication of damaged DNA [46].

The kinase ATR is often activated by oncogenic stresses and may also have unique targets particularly those functioning in pathways connected to replication fork repair as the Fanconi anemia (FA) pathway. The differential methylation analysis also revealed other components of FA such as FANCA which is involved in the monoubiquitination process, which allows FANCD2 to localize to nuclear foci and interact with other sheltering proteins such as BRCA1, playing a crucial role in homologous recombination [47]. In tumors with increased levels of replicative stress, such as those with BRCA1/BRCA2 defects, the ATR inhibition not only leads to the collapse of replication forks, but also the loss of the G2-M checkpoint, promoting cell death [48, 49]. ATR inhibition has shown promising antitumor activity in preclinical models, and several ATR inhibitors (ATRi) are in clinical development as antitumor agents, especially in combination with PARP (PARPi-ATR) in BRCA1/2 deficiency [50, 51].

Finally, we found the hypomethylation of PARP4 which could be involved in the DNA repair pathway [52], but little is known about its biological function. In a recent study, however, significantly increased expression of PARP4 was observed in cisplatin-resistant ovarian cancer cell lines compared with susceptible ones. The increased expression of PARP4 in cisplatin-resistant cell lines was associated with hypomethylation of specific CpG sites in the PARP4 promoter (cg18582260 and cg17117459) and could be so an effective diagnostic biomarker to predict the response to cisplatin in ovarian cancer patients [53].

Some limitations must be considered. Although the small amount of starting plasma is efficient for classifying tumors from healthy controls, an increase in plasma amount would lead to a higher content of circulating tumor DNA that can be more informative. Moreover, our

sample size was limited which probably led to breast cancer subtype-based analyses that were not significant. An increase of the cohort of patients especially in patients with breast cancers not carrying mutations in BRCA1/2 genes is underway to perform not only a description of the methylation profile in BRCA germline breast cancer but to perform a comparative analysis with breast cancer patients without mutations.

## Conclusions

We focused on identifying a methylation profile in patients with breast cancers characterized by the presence of germline mutations in BRCA1 or BRCA2. DMRs were most related to genes involved in the process of signal transduction mediated by Rho/Ras GTPase activity and dysregulated RNA polymerase II promoter-proximal pausing and DNA repair mechanisms.

Finally, the classifier based on these differentially methylated regions was able to classify breast cancers carrying BRCA germline mutations from healthy controls with high accuracy and sensitivity.

## Abbreviations

cfDNA	Circulating free DNA
DMR	Differentially methylated regions
cfMeDIP-seq	Cell-free methylated DNA immunoprecipitation and high-throughput sequencing
ER	Estrogen Receptors
TF	Transcription factors
PARP	Poly [ADP-ribose] polymerase
PARP-1	Poly [ADP-ribose] polymerase 1
TCGA	The Cancer Genome Atlas Program
PCA	Principal component analysis
BC	Breast cancer
HRR	Homologous recombination repair
TF	Transcription factor
TSS	Transcription start site
DNA-PK	DNA-dependent protein kinase

## Supplementary Information

The online version contains supplementary material available at <https://doi.org/10.1186/s12967-024-05734-2>.

Supplementary Material 1

Supplementary Material 2

## Acknowledgements

Research reported in this publication was performed in part at the Biostatistics and Bioinformatics Shared Resource of the Sylvester Comprehensive Cancer Center at the University of Miami, RRID: SCR\_022890, which is supported by the National Cancer Institute (NCI) of the National Institutes of Health (NIH) under award number P30CA240139. The content is solely the responsibility of the authors and does not necessarily represent the official views of the NIH.

## Author contributions

Conceptualization: (Michele Ceccarelli), M.C (Michele Caraglia) and M.O (Michele Orditura) recruited patients and data: R.A(Raffaele Addeo), F.C(Francesca Carlino), A.M.C(Alessia Maria Cossu), Stefano Forte(S.F), Raffaella Giuffrida(R.G), Anna Ceccarelli(A.C) Methodology: P.G(Piera Grisolia), R.T(Rossella Tufano), C.G(Cinzia Graziano), P.V.N (Pier Vitale Nuzzo), M.B(Marco Bocchetti), M.S(Marianna Scrima), Francesco Caraglia(F.C) Analysis: R.T. and P.G. Writing: P.G and R.T. Supervision: M.C. and M.C.

**Funding**

This study was supported by Ministero delle Imprese e del Made in Italy (MIMIT) for the Epi-Met project “Epi-MET—Funzionalizzazione delle aberrazioni (epi)genomiche nei tumori metastatici”, grant number: F/310034/01–03/X56.

**Data availability**

Data supporting the figures generated are available from authors under reasonable request.

**Declarations****Ethics approval and consent to participate**

The study was approved by the Ethics Committee of University of Campania “Luigi Vanvitelli” - Azienda Ospedaliera Universitaria “Luigi Vanvitelli” - AORN “Ospedali dei Colli” (Approval number: 133449 on 29th April 2021). Informed consent was obtained from all patients.

**Consent for publication**

Not applicable.

**Competing interests**

All authors declare that they have no conflict of interest.

**Author details**

<sup>1</sup>Sylvester Comprehensive Cancer Center and Department of Public Health Sciences, Miller School of Medicine, University of Miami, Miami, FL, USA

<sup>2</sup>Laboratory of Molecular and Precision Oncology, Biogem, IRGS, Ariano Irpino, Italy

<sup>3</sup>Laboratory of Computational Biology, IRGS, Ariano Irpino, Italy

<sup>4</sup>Department of Precision Medicine, University of Campania “Luigi Vanvitelli”, Via L. De Crecchio, 7, 80138 Naples, Italy

<sup>5</sup>Oncology Unit, San Felice a Cancelli Hospital, ASL Caserta, Sanfelice a Cancelli, Italy

<sup>6</sup>Oncology Unit, S. Giovanni di Dio Hospital, ASL Napoli2 Nord, Frattamaggiore, Italy

<sup>7</sup>Medical Oncology, Catholic University of the Sacred Heart, 00168 Rome, RM, Italy

<sup>8</sup>Department of Pathology and Laboratory Medicine, Weill Cornell Medicine, New York, NY 10065, USA

<sup>9</sup>IOM Ricerca, Viagrande, Italy

Received: 26 June 2024 / Accepted: 5 October 2024

Published online: 15 October 2024

**References**

- Prat A, Pineda E, Adamo B, Galván P, Fernández A, Gaba L, et al. Clinical implications of the intrinsic molecular subtypes of breast cancer. *Breast*. 2015;24(Suppl 2):S26–35.
- Mijic S, Zellweger R, Chappidi N, Berti M, Jacobs K, Mutreja K, et al. Replication fork reversal triggers fork degradation in BRCA2-defective cells. *Nat Commun*. 2017;8(1):859.
- Burgess M, Puhalla S. BRCA 1/2-Mutation related and sporadic breast and ovarian cancers: more alike than different. *Front Oncol*. 2014;4:19.
- Baretta Z, Mocellin S, Goldin E, Olopade OI, Huo D. Effect of BRCA germline mutations on breast cancer prognosis: a systematic review and meta-analysis. *Med (Baltim)*. 2016;95(40):e4975.
- Wan A, Zhang G, Ma D, Zhang Y, Qi X. An overview of the research progress of BRCA gene mutations in breast cancer. *Biochim Biophys Acta Rev Cancer*. 2023;1878(4):188907.
- Luo H, Wei W, Ye Z, Zheng J, Xu R-H. Liquid biopsy of methylation biomarkers in cell-free DNA. *Trends Mol Med*. 2021;27(5):482–500.
- Li S, Tollefsbol TO. DNA methylation methods: global DNA methylation and methylomic analyses. *Methods*. 2021;187:28–43.
- Flanagan JM, Cocciardi S, Waddell N, Johnstone CN, Marsh A, Henderson S, et al. DNA methylome of familial breast cancer identifies distinct profiles defined by mutation status. *Am J Hum Genet*. 2010;86(3):420–33.
- Suijkerbuijk KPM, Fackler MJ, Sukumar S, van Gils CH, van Laar T, van der Wall E, et al. Methylation is less abundant in BRCA1-associated compared with sporadic breast cancer. *Ann Oncol*. 2008;19(11):1870–4.
- Fanale D, Pivetti A, Cancelliere D, Spera A, Bono M, Fiorino A, et al. BRCA1/2 variants of unknown significance in hereditary breast and ovarian cancer (HBOC) syndrome: looking for the hidden meaning. *Crit Rev Oncol Hematol*. 2022;172:103626.
- Flower KJ, Shenker NS, El-Bahrawy M, Goldgar DE, Parsons MT, KConFab I, et al. DNA methylation profiling to assess pathogenicity of BRCA1 unclassified variants in breast cancer. *Epigenetics*. 2015;10(12):1121–32.
- Liu MC, Oxnard GR, Klein EA, Swanton C, Seiden MV, CCGA Consortium. Sensitive and specific multi-cancer detection and localization using methylation signatures in cell-free DNA. *Ann Oncol*. 2020;31(6):745–59.
- Liu J, Zhao H, Huang Y, Xu S, Zhou Y, Zhang W, et al. Genome-wide cell-free DNA methylation analyses improve accuracy of non-invasive diagnostic imaging for early-stage breast cancer. *Mol Cancer*. 2021;20(1):36.
- Nuzzo PV, Berchuck JE, Korthauer K, Spisak S, Nassar AH, Abou Alaiwi S, et al. Detection of renal cell carcinoma using plasma and urine cell-free DNA methylomes. *Nat Med*. 2020;26(7):1041–3.
- Chen S, Petricca J, Ye W, Guan J, Zeng Y, Cheng N, et al. The cell-free DNA methylome captures distinctions between localized and metastatic prostate tumors. *Nat Commun*. 2022;13(1):6467.
- Cheng N, Skead K, Ouellette T, Bratman S, De Carvalho D, Soave D et al. Early signatures of breast cancer up to seven years prior to clinical diagnosis in plasma cell-free DNA methylomes. *Res Sq*. 2022.
- Ewels P, Magnusson M, Lundin S, Käller M. MultiQC: summarize analysis results for multiple tools and samples in a single report. *Bioinformatics*. 2016;32(19):3047–8.
- Langmead B, Salzberg SL. Fast gapped-read alignment with Bowtie 2. *Nat Methods*. 2012;9(4):357–9.
- Li H, Handsaker B, Wysoker A, Fennell T, Ruan J, Homer N, et al. The sequence Alignment/Map format and SAMtools. *Bioinformatics*. 2009;25(16):2078–9.
- Adalsteinsson VA, Ha G, Freeman SS, Choudhury AD, Stover DG, Parsons HA, et al. Scalable whole-exome sequencing of cell-free DNA reveals high concordance with metastatic tumors. *Nat Commun*. 2017;8(1):1324.
- Lienhard M, Grimm C, Morkel M, Herwig R, Chavez L. MEDIPS: genome-wide differential coverage analysis of sequencing data derived from DNA enrichment experiments. *Bioinformatics*. 2014;30(2):284–6.
- Cavalcante RG, Sartor MA. Annotatr: genomic regions in context. *Bioinformatics*. 2017;33(15):2381–3.
- Colaprico A, Silva TC, Olsen C, Garofano L, Cava C, Garolini D, et al. TCGA-biolinks: an R/Bioconductor package for integrative analysis of TCGA data. *Nucleic Acids Res*. 2016;44(8):e71.
- Heinz S, Benner C, Spann N, Bertolino E, Lin YC, Laslo P, et al. Simple combinations of lineage-determining transcription factors prime cis-regulatory elements required for macrophage and B cell identities. *Mol Cell*. 2010;38(4):576–89.
- Alvarez MJ, Shen Y, Giorgi FM, Lachmann A, Ding BB, Ye BH, et al. Functional characterization of somatic mutations in cancer using network-based inference of protein activity. *Nat Genet*. 2016;48(8):838–47.
- Lachmann A, Giorgi FM, Lopez G, Califano A. ARACNe-AP: gene network reverse engineering through adaptive partitioning inference of mutual information. *Bioinformatics*. 2016;32(14):2233–5.
- Sing T, Sander O, Beerenwinkel N, Lengauer T. ROCr: visualizing classifier performance in R. *Bioinformatics*. 2005;21(20):3940–1.
- Youden WJ. Index for rating diagnostic tests. *Cancer*. 1950;3(1):32–5.
- Wang D, Qian X, Rajaram M, Durkin ME, Lowy DR. DLC1 is the principal biologically-relevant down-regulated DLC family member in several cancers. *Oncotarget*. 2016;7(29):45144–57.
- Zhang Y, Li Y, Wang Q, Su B, Xu H, Sun Y, et al. Role of RASA1 in cancer: a review and update (review). *Oncol Rep*. 2020;44(6):2386–96.
- Lone SN, Nisar S, Masoodi T, Singh M, Rizwan A, Hashem S, et al. Liquid biopsy: a step closer to transform diagnosis, prognosis and future of cancer treatments. *Mol Cancer*. 2022;21(1):79.
- Kim A, Mo K, Kwon H, Choe S, Park M, Kwak W et al. Epigenetic regulation in breast cancer: insights on epidrugs. *Epigenomes*. 2023;7(1).
- Hansen KD, Timp W, Bravo HC, Sabuncyan S, Langmead B, McDonald OG, et al. Increased methylation variation in epigenetic domains across cancer types. *Nat Genet*. 2011;43(8):768–75.
- Zhang X, Zhao D, Yin Y, Yang T, You Z, Li D, et al. Circulating cell-free DNA-based methylation patterns for breast cancer diagnosis. *NPJ Breast Cancer*. 2021;7(1):106.

35. Cristall K, Bidard F-C, Pierga J-Y, Rauh MJ, Popova T, Sebbag C, et al. A DNA methylation-based liquid biopsy for triple-negative breast cancer. *NPJ Precis Oncol.* 2021;5(1):53.
36. Widschwendter M, Evans I, Jones A, Ghazali S, Reisel D, Ryan A, et al. Methylation patterns in serum DNA for early identification of disseminated breast cancer. *Genome Med.* 2017;9(1):115.
37. Nassiri F, Chakravarthy A, Feng S, Shen SY, Nejad R, Zuccato JA, et al. Detection and discrimination of intracranial tumors using plasma cell-free DNA methylomes. *Nat Med.* 2020;26(7):1044–7.
38. Liu G, Huang S, Ailles L, Rey-McIntyre K, Melton C, Shen S et al. Clinical validation of a tissue-agnostic genome-wide methylome enrichment MRD assay for head and neck malignancies. *Ann Oncol.* 2024.
39. Dubois F, Bergot E, Zalcmán G, Levallet G. RASSF1A, puppeteer of cellular homeostasis, fights tumorigenesis, and metastasis—an updated review. *Cell Death Dis.* 2019;10(12):928.
40. Legrand AJ, Choul-Li S, Spriet C, Idziorek T, Vicogne D, Drobecq H, et al. The level of Ets-1 protein is regulated by poly(ADP-ribose) polymerase-1 (PARP-1) in cancer cells to prevent DNA damage. *PLoS ONE.* 2013;8(2):e55883.
41. Choul-Li S, Legrand AJ, Bidon B, Vicogne D, Villeret V, Aumercier M. Ets-1 interacts through a similar binding interface with Ku70 and poly (ADP-Ribose) Polymerase-1. *Biosci Biotechnol Biochem.* 2018;82(10):1753–9.
42. Legrand AJ, Choul-Li S, Villeret V, Aumercier M. Poly(ADP-ribose) Polymerase-1 (PARP-1) inhibition: a promising therapeutic strategy for ETS-Expressing Tumours. *Int J Mol Sci.* 2023;24(17).
43. Brysbaert G, de Ruyck J, Aumercier M, Lensink MF. Identification of Novel Interaction partners of Ets-1: focus on DNA repair. *Genes.* 2019;10(3).
44. Chatterjee N, Walker GC. Mechanisms of DNA damage, repair, and mutagenesis. *Environ Mol Mutagen.* 2017;58(5):235–63.
45. Alblihy A, Shoqafi A, Toss MS, Algethami M, Harris AE, Jeyapalan JN, et al. Untangling the clinicopathological significance of MRE11-RAD50-NBS1 complex in sporadic breast cancers. *NPJ Breast Cancer.* 2021;7(1):143.
46. Blackford AN, Jackson SP, ATM, ATR. The trinity at the heart of the DNA damage response. *Mol Cell.* 2017;66(6):801–17.
47. D'Andrea AD. Susceptibility pathways in Fanconi's anemia and breast cancer. *N Engl J Med.* 2010;362(20):1909–19.
48. Gralewska P, Gajek A, Marczak A, Rogalska A. Participation of the ATR/CHK1 pathway in replicative stress targeted therapy of high-grade ovarian cancer. *J Hematol Oncol.* 2020;13(1):39.
49. Huntoon CJ, Flatten KS, Wahner Hendrickson AE, Huehls AM, Sutor SL, Kaufmann SH, et al. ATR inhibition broadly sensitizes ovarian cancer cells to chemotherapy independent of BRCA status. *Cancer Res.* 2013;73(12):3683–91.
50. Kim H, Xu H, George E, Hallberg D, Kumar S, Jagannathan V, et al. Combining PARP with ATR inhibition overcomes PARP inhibitor and platinum resistance in ovarian cancer models. *Nat Commun.* 2020;11(1):3726.
51. Yazinski SA, Comaills V, Buisson R, Genois M-M, Nguyen HD, Ho CK, et al. ATR inhibition disrupts rewired homologous recombination and fork protection pathways in PARP inhibitor-resistant BRCA-deficient cancer cells. *Genes Dev.* 2017;31(3):318–32.
52. Cirello V, Colombo C, Pogliaghi G, Proverbio MC, Rossi S, Mussani E, et al. Genetic variants of PARP4 gene and PARP4P2 pseudogene in patients with multiple primary tumors including thyroid cancer. *Mutat Res.* 2019;816–818:111672.
53. Sung HY, Han J, Chae YJ, Ju W, Lee Kang J, Park AK, et al. Identification of a novel PARP4 gene promoter CpG locus associated with cisplatin chemoresistance. *BMB Rep.* 2023;56(6):347–52.

#### Publisher's note

Springer Nature remains neutral with regard to jurisdictional claims in published maps and institutional affiliations.